INTERNATIONAL JOURNAL FOR NUMERICAL METHODS IN FLUIDS
Int. J. Numer. Meth. Fluids 2000; **34**: 31–46

Large eddy simulation of free surface shallow-water flow

C. W. Li* and J. H. Wang

Department of Civil and Structural Engineering, The Hong Kong Polytechnic University, Kowloon, Hong Kong SAR, People's Republic of China

SUMMARY

Shallow-water flow with free surface frequently occurs in ambient water bodies, in which the horizontal scale of motion is generally two orders of magnitude greater than the water depth. To accurately predict this flow phenomenon in more detail, a three-dimensional numerical model incorporating the method of large eddy simulation (LES) has been developed and assessed. The governing equations are split into three parts in the finite difference solution: advection, dispersion and propagation. The advection part is solved by the QUICKEST scheme. The dispersion part is solved by the central difference method and the propagation part is solved implicitly using the Gauss–Seidel iteration method. The model has been applied to free surface channel flow for which ample experimental data are available for verification. The inflow boundary condition for turbulence is generated by a spectral line processor. The computed results compare favourably with the experimental data and those results obtained by using a periodic boundary condition. The performance of the model is also assessed for the case in which anisotropic grids and filters with horizontal grid size of the order of the water depth are used for computational efficiency. The coarse horizontal grid was found to cause a significant reduction in the large-scale turbulent motion generated by the bottom turbulence, and the turbulent motion is predominately described by the sub-grid scale (SGS) terms. The use of the Smagorinsky model for SGS turbulence in this situation is found inappropriate. A parabolic mixing length model, which accounts for the filtered turbulence, is then proposed. The new model can reproduce more accurately the flow quantities. Copyright © 2000 John Wiley & Sons, Ltd.

KEY WORDS: free surface; large eddy simulation; shallow water; turbulence modelling

1. INTRODUCTION

The turbulence induced in ambient shallow-water bodies can be divided into two scales. The vertical scale of turbulence in the order of the water depth is mainly due to bottom friction. The lateral scale of turbulence in the order of the horizontal dimension of the water body is mainly due to flow separation and other horizontal shear flow phenomena. As the horizontal scale of motion is significantly larger than the vertical scale of motion, the hydrostatic pressure

* Correspondence to: Department of Civil and Structural Engineering, The Hong Kong Polytechnic University, Hung Hom, Kowloon, Hong Kong SAR, People's Republic of China.

Received November 1998
Revised September 1999

assumption is valid and the vertical momentum equation can be simplified. Owing to the presence of bottom friction, and occasionally wind forcing and density stratification, the flow field will be three dimensional.

For the modelling of turbulence, there are practically two approaches: large eddy simulation (LES) and turbulence models for solving the Reynolds-averaged Navier–Stokes (RANS) equations. A comparison of the two approaches indicates that LES is superior to the RANS method using turbulence models when the flow is very complex and the large-scale structures dominate the turbulent transport and/or unsteady processes are involved [1]. In terms of computational effort, LES is usually much more expensive than turbulence models for RANS. This is because LES requires a significantly larger number of time steps for statistical averaging. However, for three-dimensional unsteady flow problems, the difference in computing effort between the two approaches is not so large if the grid sizes used in the two approaches are similar.

LES is by definition three dimensional. In simulating complex flow phenomena, the specification of boundary and initial conditions needs special attention. The treatment of the free surface boundary condition is difficult, and free surface flow problems are relatively seldom tackled by the method of LES. In free surface shallow-water flow, one approach is to use the rigid-lid assumption [2]. Another approach is to account for the variation of the free water surface by vertically integrating the continuity equation, and relate the variation of the free water surface to the pressure gradient through the hydrostatic pressure assumption [3]. In ambient water bodies, the large disparity in horizontal and vertical scale of motion renders the use of LES to be expensive if the vertical scale is also computed. Bedford and Babajimopoulos [4] applied LES to a lake model and used a grid with a horizontal size two orders of magnitude greater than the vertical size. It was found that the model propagated energy inputs according to two-dimensional turbulence theory. However, the problem of using anisotropic grids and filters in shallow-water flows has not been further pursued.

In the present work, an LES model is developed for the simulation of free surface shallow-water flow. An operator splitting method is used so that different numerical schemes can be used to approximate different physical processes (e.g. Li and Yu [5]). The governing equations are split into three parts in the solution: advection, dispersion and propagation. In the advection part, the advective accelerations are approximated by the third-order QUICKEST scheme [6]. In the dispersion step, the sub-grid scale (SGS) terms are solved by central difference and the Leonard terms [7] are solved by third-order difference. In the propagation step, the surface elevation (pressure) is obtained from the solution of the Poisson-type equation. The use of anisotropic grid and filters, which are unavoidable for computational efficiency, and their effect on the computed results will be investigated. The adequacy of using the Smagorinsky model to model SGS turbulence in this situation will be studied. The model will be tested against the extensive laboratory measurements for free surface channel flows.

2. GOVERNING EQUATIONS

Denoting the velocity field by a Cartesian vector U_i, the pressure by P, the kinematic viscosity by ν (assumed constant), the density by ρ (assumed constant), the space vector by x_i, the time

by t and the spatially filtered variable by an overbar, the filtered Navier–Stokes equations for fluid motion are written as

$$\frac{\partial \bar{U}_i}{\partial x_i} = 0 \tag{1}$$

$$\frac{\partial \bar{U}_i}{\partial t} + \frac{\partial (\overline{U_i U_j})}{\partial x_j} = -\frac{1}{\rho}\frac{\partial \bar{p}}{\partial x_i} + \nu \frac{\partial^2 \bar{U}_i}{\partial x_i \partial x_j} \tag{2}$$

The non-linear adective term can be expanded as

$$\overline{U_i U_j} = (\overline{\bar{U}_i + u_i'})(\overline{\bar{U}_j + u_j'}) = \overline{\bar{U}_i \bar{U}_j} + \overline{\bar{U}_i u_j'} + \overline{u_i' \bar{U}_j} + \overline{u_i' u_j'} = \overline{\bar{U}_i \bar{U}_j} + R_{ij} \tag{3}$$

where $u_i' = U_i - \overline{U_i}$ is the velocity fluctuation. The first term represents the large-scale components and is decomposed by a Taylor series expansion of the filter convolved with the product.

$$\overline{\bar{U}_i \bar{U}_j} = \bar{U}_i \bar{U}_j + \frac{\Delta_k}{4\gamma}\frac{\partial^2}{\partial x_k^2}(\bar{U}_i \bar{U}_j) \tag{4}$$

The cross-product terms are subsumed into the SGS components and their summation is denoted by R_{ij}

$$R_{ij} = \tau_{ij} + \frac{1}{3}\delta_{ij} R_{kk} \tag{5}$$

The SGS stress is decomposed into the sum of a trace-free tensor τ_{ij} and a diagonal tensor R_{kk}, which are absorbed into the pressure term. The trace-free tensor is usually closed by the Smagorinsky eddy viscosity model [8]

$$\tau_{ij} = -\nu_T\left(\frac{\partial \bar{U}_i}{\partial x_j} + \frac{\partial \bar{U}_j}{\partial x_i}\right) = -2\nu_T S_{ij} \tag{6}$$

$$\nu_T = L^2\sqrt{2S_{ij}S_{ij}} \tag{7}$$

$$L = C_s\left[1 - \exp\left(-\frac{x_k^+}{A^+}\right)\right](\Delta_1\Delta_2\Delta_3)^{1/3} \tag{8}$$

where ν_T is an eddy viscosity, L is the turbulence characteristic length scale and is modified by the van Driest damping (with parameters x_k^+ and A^+ [9]) to account for the effects of solid wall boundaries, C_s is a constant and taken to be 0.15, $\Delta_i = 2\Delta x_i$, and Δx_i is the grid size in the ith direction. However, when a coarse grid is used, the adequacy of using the Smagorinsky eddy viscosity model has to be investigated.

By assuming hydrostatic pressure, the filtered equations of motions become

$$\frac{\partial \bar{U}_i}{\partial t}+\frac{\partial\left(\bar{U}_i\bar{U}_j+\dfrac{\Delta_k}{4\gamma}\dfrac{\partial^2}{\partial x_k^2}(\bar{U}_i\bar{U}_j)\right)}{\partial x_j}=-\frac{1}{\rho}\frac{\partial \bar{P}}{\partial x_i}+\nu\frac{\partial^2\bar{U}_i}{\partial x_i\,\partial x_j}-\frac{\partial(-2\nu_T S_{ij})}{\partial x_j},\quad i=1,2 \tag{9}$$

$$\frac{\partial \bar{P}}{\partial x_3}=-\rho g \tag{10}$$

The vertical velocity is obtained from the continuity equation

$$\frac{\partial \bar{U}_3}{\partial x_3}=-\frac{\partial \bar{U}_1}{\partial x_1}-\frac{\partial \bar{U}_2}{\partial x_2} \tag{11}$$

The variation of free surface is obtained from the hydrostatic pressure equation and the continuity equation

$$\frac{\partial \eta}{\partial t}=-\frac{\partial}{\partial x_1}\int_{-h}^{\eta}\bar{U}_1\,\mathrm{d}x_3-\frac{\partial}{\partial x_2}\int_{-h}^{\eta}\bar{U}_2\,\mathrm{d}x_3 \tag{12}$$

where $\eta(x_1, x_2)$ is the surface elevation and $x_3=-h$ represents the bottom. The surface elevation is related to the pressure at $x_3=0$, $P_0=P(x_1, x_2, 0)$ by

$$\frac{\partial P_0}{\partial x_i}=\rho g\frac{\partial \eta}{\partial x_i},\quad i=1,2 \tag{13}$$

3. SOLUTION METHOD

The split operator approach is used in the solution of the governing equations. At each time step the equations are split into three steps: advection, diffusion and propagation. The equations for the advection step are

$$\frac{\bar{U}_i^{n+1/3}-\bar{U}_i^n}{\Delta t}=-\bar{U}_j\frac{\partial \bar{U}_i}{\partial x_j},\quad i=1,2 \tag{14}$$

The QUICKEST scheme [6] is used to solve the equations of pure advection. The scheme is third-order accurate and can eliminate the second-order numerical diffusion. A similar scheme has been analysed and applied in LES by other investigators [10]. The equations for the diffusion step are

$$\frac{\bar{U}_i^{n+2/3}-\bar{U}_i^{n+1/3}}{\Delta t}=\nu\frac{\partial^2\bar{U}_i}{\partial x_i\,\partial x_j}-\frac{\partial(-2\nu_T S_{ij})}{\partial x_j}-\frac{\partial\left(\dfrac{\Delta_k}{4\gamma}\dfrac{\partial^2}{\partial x_k^2}(\bar{U}_i\bar{U}_j)\right)}{\partial x_j},\quad i=1,2 \tag{15}$$

In the diffusion step, the simple four-node centred space scheme is used for the second-order diffusion terms and a third-order difference scheme is used for the Leonard terms (the last

terms on the right-hand side of the above equation). The equations for the propagation step are

$$\frac{\eta^{n+1}-\eta^{n+2/3}}{\Delta t}=-\frac{\partial}{\partial x_1}\int_{-h}^{\eta}\bar{U}_1\,\mathrm{d}x_3-\frac{\partial}{\partial x_2}\int_{-h}^{\eta}\bar{U}_2\,\mathrm{d}x_3 \tag{16}$$

$$\frac{\partial \bar{U}_i}{\partial t}=-g\frac{\partial \eta}{\partial x_i},\quad i=1,2 \tag{17}$$

Equation (17) is due to the surface elevation not being level. Equations (16) and (17) are solved implicitly. The three equations are decoupled through two procedures. Firstly, the unknown flow rates at time step $n+1$ are eliminated by differentiating Equation (17) with respect to x (x_1) and y (x_2). Secondly, the resulting Poisson-type equation with an essential boundary condition is solved by using the Gauss–Seidel iteration method. Finally, the vertical velocity U_3 is computed from the continuity equation

$$U_3=-\int_{-h}^{x_3}\left(\frac{\partial U_1}{\partial x_1}+\frac{\partial U_2}{\partial x_2}\right)\mathrm{d}x_3 \tag{18}$$

4. BOUNDARY CONDITIONS

The specification of boundary condition is difficult in the LES model because the turbulence quantities need to be specified. Periodic boundary condition (PBC) is predominately used at the inflow boundary for its easiness of implementation [2,11]. This type of boundary condition is appropriate for the case that the inflow condition and the outflow condition are identical. However, in more complicated situations, frequently occurring in engineering problems, such as flow in an expanding or converging channel, PBC cannot be used. Another more general approach is to specify the inflow quantities. For free surface shallow-water flow, the vertical variation of the filtered longitudinal velocity U ($\equiv U_1$) can be specified as a logarithmic profile [12] with a Manning coefficient n and the transverse filtered velocities, V ($\equiv U_2$) and W ($\equiv U_3$), can be assumed equal to zero and the water depth can be extrapolated from the interior points (zero gradients). Turbulence quantities at the inflow boundary can be generated by a spectral line processor (SLP) [13]. This is achieved by firstly specifying the initial $u'(x, y, z, 0)$, $v'(x, y, z, 0)$, $w'(x, y, z, 0)$; $u'\equiv u'_1$, $v'\equiv u'_2$, $w'\equiv u'_3$. The expression is given by

$$\begin{aligned}u'(x,y,z,0)=\sqrt{2}\sum_{j_1=1}^{N_1}\sum_{j_2=1}^{N_2}\sum_{j_3=1}^{N_3}&[E_x(\omega_{xj_1},\omega_{yj_2},\omega_{zj_3})\Delta\omega_x\Delta\omega_y\Delta\omega_z]^{1/2}\\&\times\cos(\omega'_{xj_1}x+\omega'_{yj_2}y+\omega'_{zj_3}z+\phi_{j_1j_2j_3})\end{aligned} \tag{19}$$

where E_x is the target spectrum, $\phi_{j_1j_2j_3}$ is the independent random phase uniformly distributed between 0 and 2π, ω_{xj_i} is the angular frequency in the x-direction ($=(j_i-1/2)\Delta\omega_x$, etc;

$\omega'_{xj_i} = \omega_{xj_i} + \delta\omega_x$, etc, where $\delta\omega_x$ is a small random frequency introduced to eliminate the periodicity of the simulated process. A similar expression can be obtained for v' and w'. The target spectra chosen are those obtained experimentally (e.g. Hinze [14]), and are given as follows:

$$E_x(k_x) = \frac{2}{\pi} u'^2 \frac{\lambda}{1 + k_x^2 \lambda^2} \tag{20}$$

$$E_y(k_x) = E_z(k_x) = \frac{2}{\pi} u'^2 \lambda \frac{1 + 3k_x^2 \lambda^2}{1 + k_x^2 \lambda^2} \tag{21}$$

where $k_x = \omega_x / U$ is the wavenumber in the main flow direction (x-direction) with mean velocity U; u'^2 is the mean squared velocity fluctuation in the x-direction; λ is a macroscale of turbulence. In free surface channel flow, Nezu and Nakagawa [15] showed that

$$\frac{\lambda}{H} = \sqrt{\frac{z}{H}}, \quad \text{for } z/H < 0.6 \tag{22a}$$

$$\frac{\lambda}{H} = 0.77, \quad \text{for } z/H > 0.6 \tag{22b}$$

where H is the water depth, z is the vertical ordinate measured from the bottom. By choosing the length of the computational domain (L_D) to be sufficiently long so that the inflow and outflow boundary conditions are uncorrelated, the inflow boundary condition can be specified using Taylor's frozen turbulence hypothesis [16]

$$u'(0, y, z, t) = u'(x', y, z, 0) \tag{23}$$

where $x' = nL_D - Ut$, n is a positive integer chosen such that $0 < x' < L_D$.

At outflow boundary, the water depth and velocities are determined from a radiation boundary condition. At the solid wall boundary, no-slip boundary condition is used and the wall function technique [17] is applied. At the water surface, the surface shear stresses τ_{sx} and τ_{sy} are set to zero. At the bottom, the magnitudes of the bottom shear stresses τ_{bx} and τ_{by} are specified by the Manning equation. Another method of relating the bed shear stress to the near wall velocity using the log law has also been tried. It was found that the computed results display not much difference.

The initial condition consists of a mean velocity and depth field, as well as a turbulence field. The vertical variation of the filtered longitudinal velocity U is specified as a logarithmic profile with a Manning coefficient n. The transverse filtered velocities, V and W, are assumed equal to zero and the water depth is computed based on force balance. The turbulence quantities are imposed to the mean velocity field and are generated by a random number generator if PBC is used, or generated by the SLP if the inflow quantities are specified.

5. MODEL ASSESSMENT

Free surface flow in a rectangular channel is used as the test case for assessing the performance of the model. The reason is that there are ample experiments being carried out and the results are consistent and conclusive [15]. The main purposes are threefold. The first is to study the performance of using different inflow boundary conditions. The second is to investigate the effect of anisotropy of grid size and filtering. The third is to assess the Smagorinsky eddy viscosity model. The major source of turbulence in this situation is from the bed shear stress at the bottom.

The dimensions of the channel section are $3.2 \times 1.6 \times 0.2$ m^3. The grid system consists of 161 grid points in the streamwise direction, 81 grid points in the transverse direction and 21 grid points in the vertical direction. The flow is sub-critical with a mean velocity of 0.5 m s^{-1} and the Reynolds number based on the depth and the mean velocity is $Re = 10^5$.

The inflow boundary conditions are studied first. In using the PBC, the dynamic steady state is attained in about four turnover periods (Figure 1). If the inflow boundary condition is generated by the SLP, the flow is found to attain dynamic steady state after only two turnover periods and the solution becomes periodic (Figure 2). The reason for the periodicity of the solution is that the initial condition is generated only for the computational domain, and the inflow boundary condition is inferred from the initial condition and hence is repetitive according to Equation (23). It is noted that the time-averaged velocities for the case of using PBC are slightly higher than those in the case of using SLP. This is probably due to that there is no control on the magnitude of the discharge rate for the case of using PBC. The amplitude

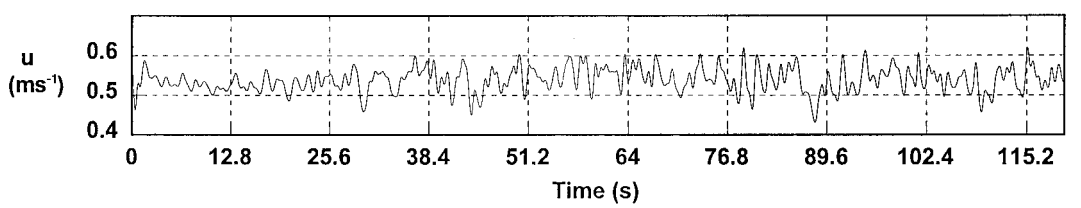

Figure 1. Time variation of u-velocity at a typical point; PBC.

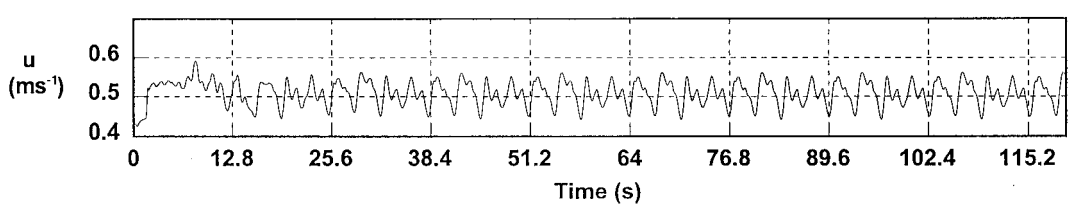

Figure 2. Time variation of u-velocity at a typical point (inflow boundary condition generated by an SLP).

of variation of the velocity fluctuations is also larger for the case of using PBC, partly due to the larger mean velocity for this case. A typical field plot of the instantaneous U-velocity is shown in Figure 3. The turbulence statistics are collected for the subsequent ten turnover periods. Figure 4 displays the mean vertical velocity profile at the centre of the computational domain. The agreement between the computed results and the measured results [15] is satisfactory for both cases. Figure 5(a)–(e) shows the distributions of the root-mean-square (rms) velocity fluctuations (u', v', w'), the turbulence kinetic energy (k) and the vertical shear stress $\overline{u'w'}$. The quantities are made non-dimensional by division with the shear velocity u^* or square of u^*, where $u^* = \sqrt{\tau_b/\rho}$, and τ_b is the bottom shear stress. The computed values with PBC are higher than the mean experimental values, while the computed values with SLP

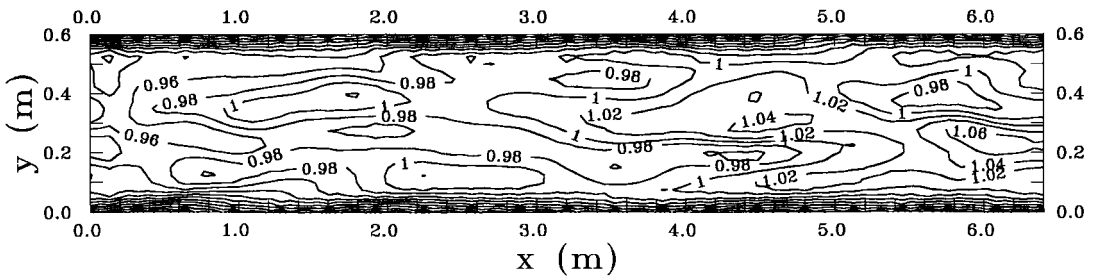

Figure 3. Field plot of the instantaneous U-velocity.

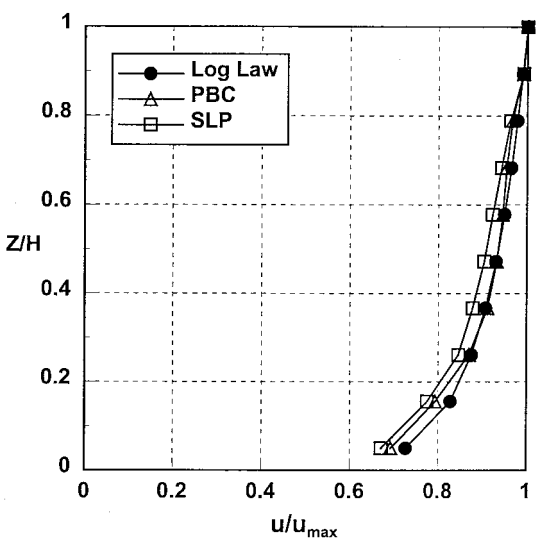

Figure 4. Mean vertical velocity profile for different inflow boundary conditions

display a smaller turbulence energy content and are closer to the mean experimental values. This shows that the imposition of the inflow boundary condition consists of the mean velocity profile and the turbulence field generated by the SLP being comparable with the widely used PBC. The implication is that in the application of the LES model to a more complicated situation, in which the PBC cannot be used, the inflow boundary condition can be specified by the SLP.

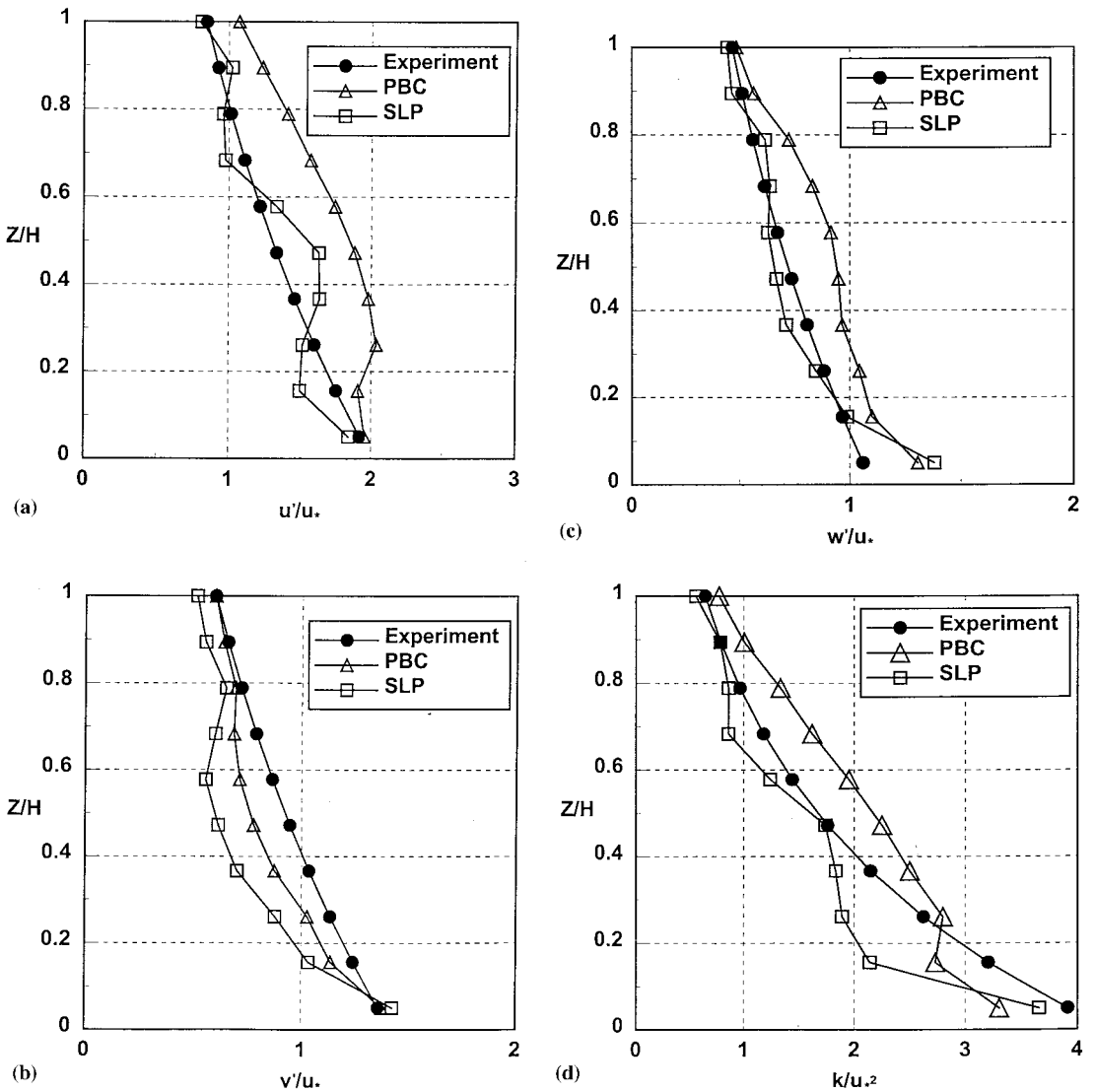

Figure 5. Vertical profiles of turbulence quantities: (a) u'; (b) v'; (c) w'; (d) k; (e) $\overline{u'w'}$.

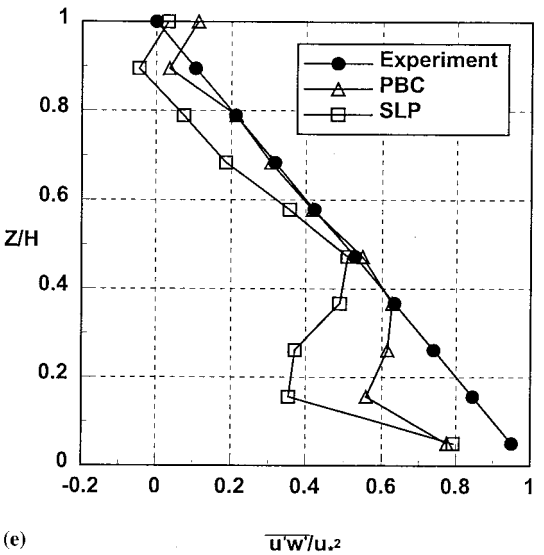

Figure 5 (*Continued*)

To investigate the effect of anisotropy of the grid size and the filtering, the number of grid points in the transverse direction is reduced to 9, and the grid size in this direction is 0.2 m, which is equal to the water depth. With such a grid size, the large-scale eddies and also the secondary recirculations are filtered out. The time variation of the u-velocity at a typical point displays no apparent fluctuation (Figure 6(a)) for the case of PBC and only a long-period fluctuation with high frequency components significantly damped for the case of using SLP (Figure 6(b)). The computed mean vertical velocity profile shows a large deviation from the logarithmic distribution for the case of PBC, and a lesser deviation for the case of using SLP (Figure 7, Smagorinsky model). The associated turbulence quantities are significantly greater than the corresponding experimental values (Figures 8 and 9, Smagorinsky model). This can be explained by the fact that the turbulence, which is mainly bottom generated, is now predominately accounted for by the SGS turbulence terms. As the size of the turbulence eddies is of the order of the water depth, the use of the horizontal grid size close to the water depth will make the SGS turbulence include the most energy containing eddies and hence the use of the Smagorinsky eddy viscosity model is inappropriate. The use of LES with a coarse grid is similar to the RANS simulation in which the turbulent motion with all scales is simulated by a turbulent closure model.

To model more accurately the SGS turbulence in a coarse grid system, a parabolic mixing length model is proposed. In this model the length scale is given by

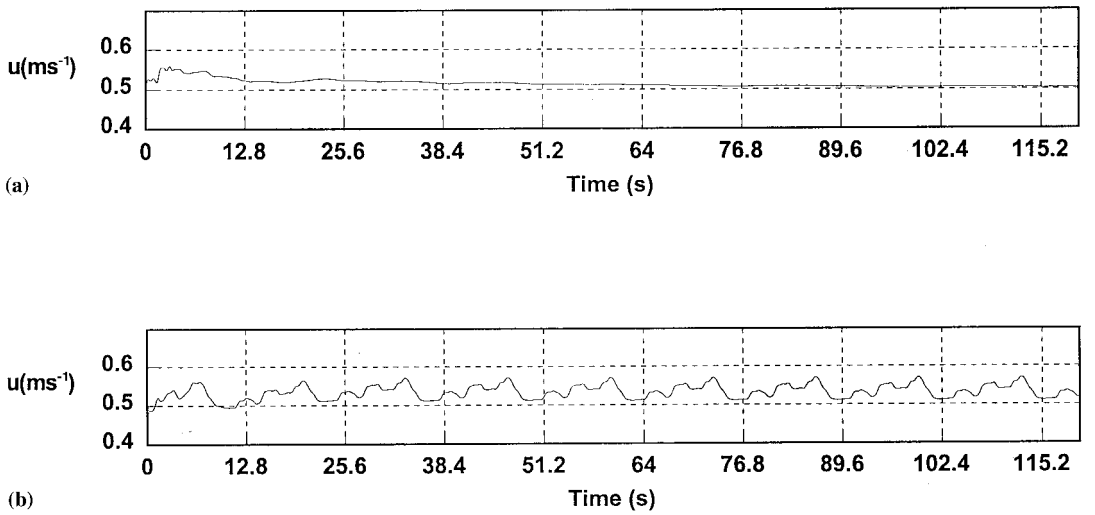

Figure 6. Time variation of u-velocity at a typical point (coarse grid): (a) PBC, (b) SLP.

$$L = \min\left(C_s\left[1 - \exp\left(-\frac{x_k^+}{A^+} \right) \right] (\Delta_x \Delta_y \Delta_z)^{1/3},\ \kappa z \left(1 - \frac{z}{H} \right) \right) \tag{24}$$

where $\Delta_x = 2\Delta x$, $\Delta_y = 2\Delta y$ and $\Delta_z = 2\Delta z$; and Δx, Δy and Δz are the grid sizes in the x-, y- and z-directions respectively. The equation describes the fact that the turbulence length scale is limited by the water depth if the gird size is greater than the water depth, and is limited by the grid size if the grid size is much smaller than the water depth. The parabolic variation in length scale in the second expression on the right-hand side of Equation (24) is derived based on the logarithmic variation of the vertical velocity profile and a linear vertical variation of the shear stress in open channel flow [18]. The expression has been verified experimentally [15]. As compared with the use of the Smagorinsky eddy viscosity model, the computed mean velocity profile shows a better agreement with the measured distribution (Figure 7). For the turbulence quantities, improvement in the prediction of the vertical shear and turbulence kinetic energy is obtained (Figures 8 and 9), especially for the case of using PBC. This is due to the specification of the correct turbulent length scale. However, the vertical variation of the turbulence kinetic energy displays a more rapid decrease in magnitude near the surface. This is mainly due to the reduction of both the length scale and the magnitude of velocity gradient near the free surface. The variation of the fluctuations of the velocity components cannot be computed directly because the

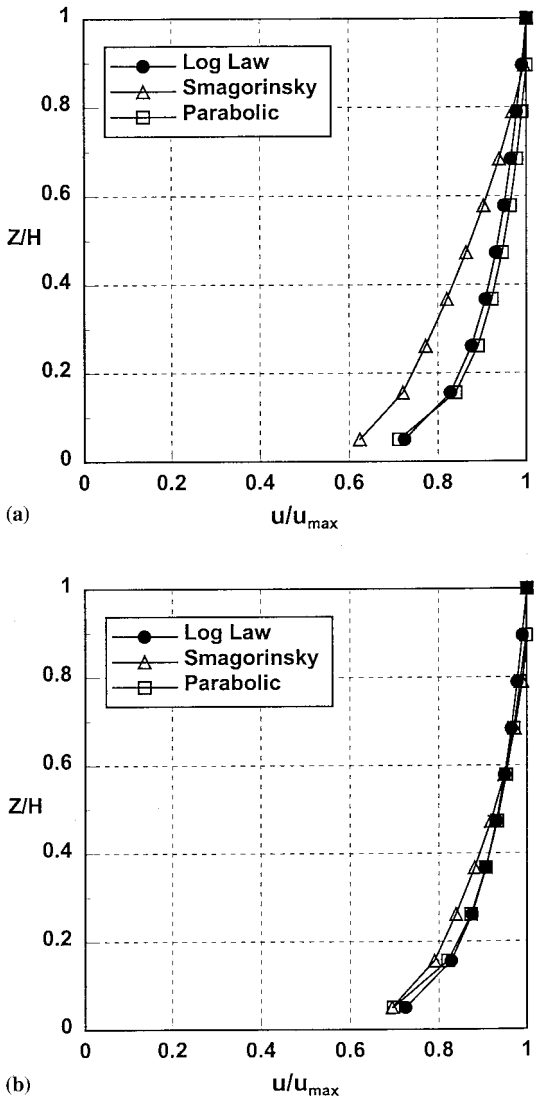

Figure 7. Mean vertical velocity profiles (coarse grid): (a) PBC; (b) SLP.

large-scale turbulence is filtered out. If the distribution of the kinetic energy is assumed to follow the ratio of 16:9:4 in the x-, y-, z-directions respectively, the results are close to those obtained empirically (Figure 10). This ratio is a good approximation for boundary layer flow.

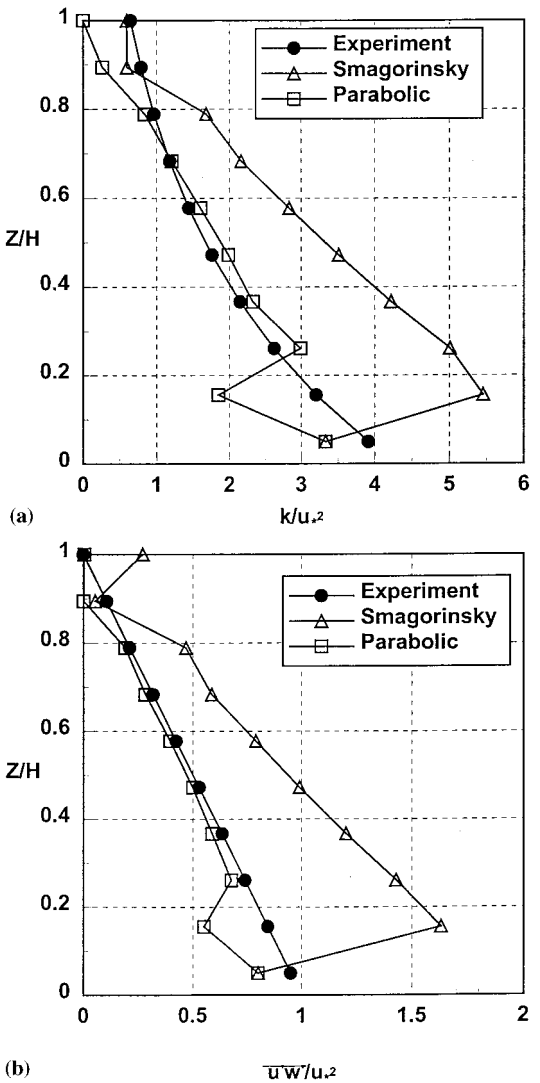

Figure 8. Vertical profiles of turbulence quantities (coarse grid, PBC): (a) k; (b) $\overline{u'w'}$.

6. CONCLUSIONS

An LES model has been developed and applied to study free surface shallow-water flow. The imposition of the inflow turbulence quantities using an SLP produces results that compare

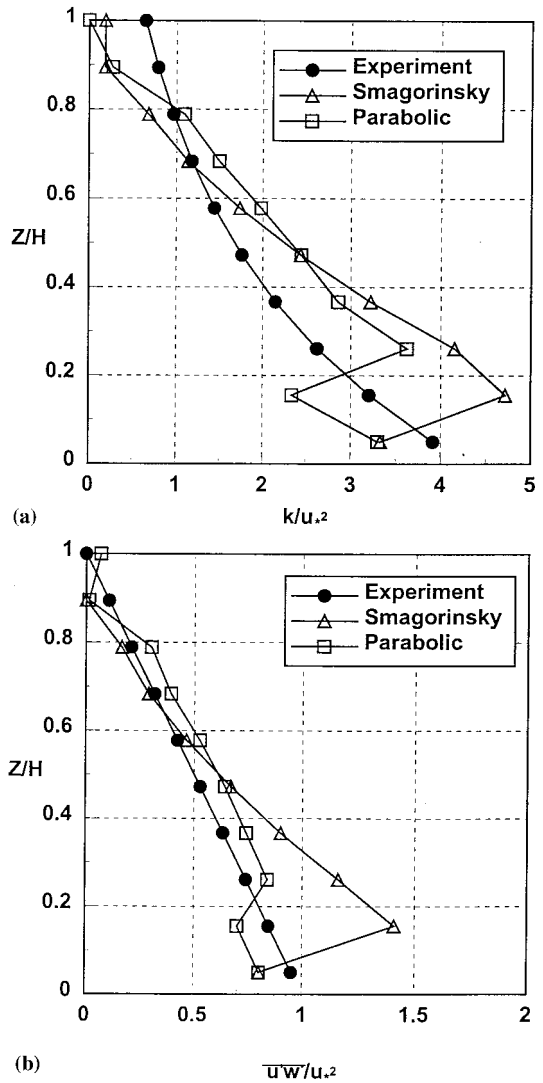

Figure 9. Vertical profiles of turbulence quantities (coarse grid, SLP): (a) k; (b) $\overline{u'w'}$.

favourably with the mean experimental results and those from the case of using periodic boundary condition. A significant reduction of the large-scale turbulence is resulted when coarse grid is used, and a parabolic mixing length model performs better than the Smagorinsky model in this situation.

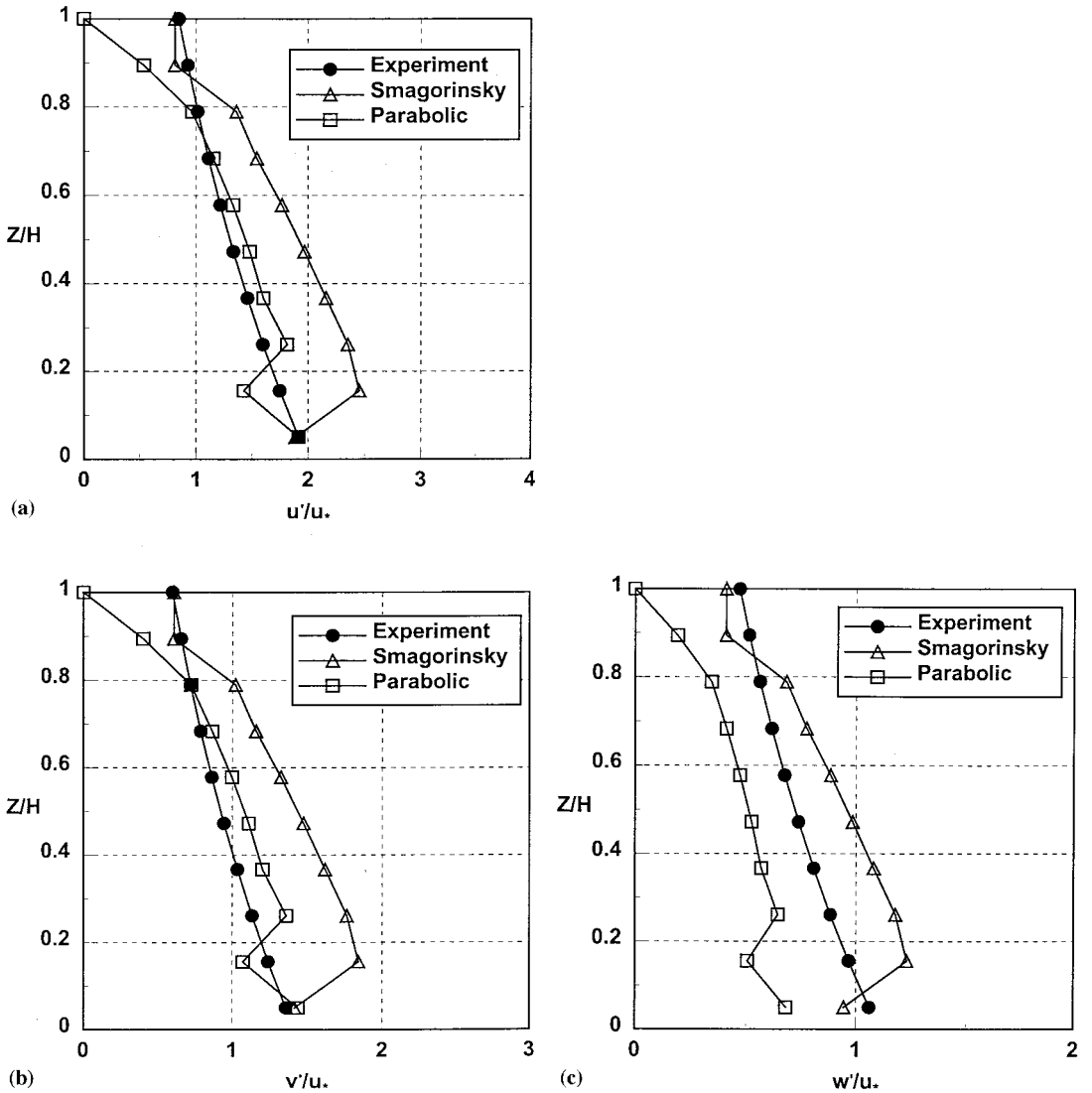

Figure 10. Vertical profiles of inferred velocity fluctuations (coarse grid, PBC): (a) u'; (b) v'; (c) w'.

ACKNOWLEDGMENTS

This work was supported by a grant from the Research Grant Council of the Hong Kong Special Administrative Region (Project No. 58/96E) and a grant from the Natural Science Foundation of China (Project No. 49676285).

REFERENCES

1. Rodi W. Large-eddy simulation and statistical turbulence models: complementary approaches. In *New Tools in Turbulence Modelling*, Metais O, Ferziger JH (eds). Springer: Berlin, 1996.
2. Thomas TG, Williams JJR. Large eddy simulation of turbulent flow in an asymmetric compound open channel. *Journal of Hydraulic Research* 1995; **33**: 27–42.
3. Babajimopoulos C, Bedford KW. Formulating lake models which preserve spectral statistics. *Journal of Hydraulics Division ASCE* 1980; **106**: 1–19.
4. Bedford KW, Babajimopoulos C. Verifying lake transport models with spectral statistics. *Journal of Hydraulics Division ASCE* 1980; **106**: 21–38.
5. Li CW, Yu TS. Numerical investigation of shallow recirculating flows by a quasi-three-dimensional k–ε model. *International Journal for Numerical Methods in Fluids* 1996; **23**: 485–501.
6. Leonard BP. A stable and accurate convective modelling procedure based on quadratic upstream interpolation. *Computational Methods in Applied Mechanical Engineering* 1979; **19**: 59–98.
7. Leonard A. Energy cascade in large-eddy simulations of turbulent fluid flows. *Advances in Geophysics* 1974; **18A**: 237–248.
8. Smagorinsky J. General circulation experiments with the primitive equations. Part I: the basic experiment. *Monthly Weather Review* 1963; **91**: 99–152.
9. Van Driest ER. On turbulent flow near a wall. *Journal of Aerospace Science* 1956; **23**: 1007–1011.
10. Ragab SA, Sheen SC. Large eddy simulation of mixing layer. In *Large Eddy Simulation of Complex Engineering and Geophysical Flows*, Galperin B, Orszag SA (eds). Cambridge University Press: Cambridge, 1993.
11. Deardorff JW. A numerical study of three-dimensional turbulent channel flow at large Reynolds numbers. *Journal of Fluid Mechanics* 1970; **41**: 453–480.
12. Nezu I, Rodi W. Open channel flow measurements with a laser Doppler anemonmeter. *Journal of Hydraulic Engineering ASCE* 1986; **112**: 101–129.
13. Shinozuka M, Jan CM. Digital simulation of random processes and its applications. *Journal of Sound and Vibration* 1972; **25**(1): 111–128.
14. Hinze JO. *Turbulence*. McGraw-Hill: New York, 1975.
15. Nezu I, Nakagawa H. *Turbulence in Open-channel Flows*. A.A. Balkema: Rotterdam, 1993.
16. Frost W. Spectral theory of turbulence. In *Handbook of Turbulence*, vol. 1. Plenum Press: New York, 1978.
17. Launder BE, Spalding DB. The numerical computation of turbulent flows. *Computational Methods in Applied Mechanical Engineering* 1974; **3**: 269–289.
18. Fischer HB, Imberger J, List EJ, Koh RCY, Brooks NH. *Mixing in Inland and Coastal Waters*. Academic Press: New York, 1979.

